



1 **The additionality problem of Ocean Alkalinity Enhancement**

2

3 Lennart T. Bach

4

5 Institute for Marine and Antarctic Studies, University of Tasmania, Hobart, TAS, Australia.

6

7 *Correspondence to:* Lennart T. Bach (Lennart.bach@utas.edu.au)

8

9

10 **Abstract.** Ocean Alkalinity Enhancement (OAE) is an emerging approach for atmospheric carbon dioxide
11 removal (CDR). The net climatic benefit of OAE depends on how much it can increase carbon sequestration
12 relative to a baseline state without OAE. This so-called ‘additionality’ can be calculated as:

13

14

$$\text{Additionality} = C_{\text{OAE}} - \Delta C_{\text{baseline}}$$

15

16 So far, feasibility studies on OAE have mainly focussed on enhancing alkalinity in the oceans (C_{OAE}) but not
17 primarily how such anthropogenic alkalinity would modify the natural alkalinity cycle ($\Delta C_{\text{baseline}}$). Here, I present
18 incubation experiments where materials considered for OAE (sodium hydroxide, steel slag, olivine) are exposed
19 to beach sand to investigate the influence of anthropogenic alkalinity on natural alkalinity sources and sinks. The
20 experiments show that anthropogenic alkalinity can strongly reduce the generation of natural alkalinity, thereby
21 reducing additionality. This is because the anthropogenic alkalinity increases the calcium carbonate saturation
22 state, which reduces the dissolution of calcium carbonate from sand, a natural alkalinity source. I argue that this
23 ‘additionality problem’ of OAE is potentially widespread and applies to many marine systems where OAE
24 implementation is considered – far beyond the beach scenario investigated in this study. However, the problem
25 can potentially be mitigated by dilute dosing of anthropogenic alkalinity into the ocean environment, especially
26 at hotspots of natural alkalinity cycling such as in marine sediments. Understanding a potential slowdown of the
27 natural alkalinity cycle through the introduction of an anthropogenic alkalinity cycle will be crucial for the
28 assessment of OAE.

29

30 **1. Introduction**

31

32 Keeping global warming between 1.5 to 2°C requires rapid reduction of greenhouse gas emissions and gigatonne-
33 scale atmospheric carbon dioxide removal (CDR), using a portfolio of terrestrial and marine CDR methods
34 (Nemet et al., 2018). Ocean alkalinity enhancement (OAE) is considered as an important CDR method of the
35 marine portfolio (Hartmann et al., 2013). OAE can be achieved through a variety of geochemical and
36 electrochemical processes (Renforth and Henderson, 2017). All of them enhance surface ocean alkalinity to
37 reduce the hydrogen ion (H^+) concentration in seawater (i.e. increase pH). This reduction in $[\text{H}^+]$ causes a shift in
38 the carbonate chemistry equilibrium:

39



41

42 from CO_2 on the left towards bicarbonate (HCO_3^-) and carbonate ion (CO_3^{2-}) on the right. The associated reduction
43 of the CO_2 partial pressure in seawater ($p\text{CO}_2$) enables atmospheric CO_2 influx into the oceans (or reduces CO_2
44 outflux if $p\text{CO}_2 > \text{atmospheric } p\text{CO}_2$). This transfer (retention) of atmospheric CO_2 into the ocean leads to an
45 increase of the dissolved inorganic carbon (DIC) concentration in seawater:



48

49 Among the widely discussed OAE approaches are coastal enhanced weathering and electrolysical acid removal
50 (Eisaman et al., 2023). Coastal Enhanced Weathering achieves alkalinity increase via the addition of pulverized
51 alkaline rocks like limestone, olivine, or alkaline industrial products like steel slag to coastal environments (Feng
52 et al., 2017; Harvey, 2008; Meysman and Montserrat, 2017; Renforth, 2019; Schuiling and Krijgsman, 2006). In
53 the case of limestone, alkalinity enhancement and CDR are generated through the dissolution of e.g. CaCO_3 :

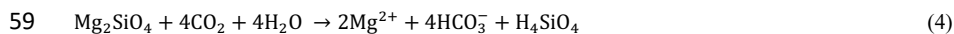
54



56

57 For olivine, alkalinity enhancement and CDR are driven predominantly by the dissolution of Forsterite (Mg_2SiO_4):

58



60

61 For steel slags, the predominant source for alkalinity contained within the material are hydroxides such as calcium
62 oxide (CaO) (Shi, 2004). Here, the net reaction of OAE and associated CDR is:

63



65

66 Electrolysical OAE is somewhat different from the above approaches since no materials are added to
67 seawater. Instead, water is split into H^+ and a hydroxide ion (OH^-) using electrical energy and electrolysical
68 membranes (de Lannoy et al., 2018). H^+ is captured as hydrochloric acid whilst OH^- is captured as sodium
69 hydroxide (NaOH). The hydrochloric acid needs to be utilised, neutralized in deep ocean sediments, or stored in
70 save reservoirs outside the ocean (Eisaman et al., 2018; Tyka et al., 2022). NaOH is enriched in the processed
71 seawater, which is released back into the surface convert CO_2 into HCO_3^- (Eisaman et al., 2018; Tyka et al., 2022):

72



74

75 A critical side-effect of OAE is the associated increase in CO_3^{2-} concentrations, which comes through the shift in
76 the marine carbonate equilibrium through H^+ absorption (see above). This increase elevates the saturation state
77 for calcium carbonate (Ω_{CaCO_3}), the metric which determines the solubility of CaCO_3 in seawater. Ω_{CaCO_3} is defined
78 as:

79



80
$$\Omega_{\text{CaCO}_3} = \frac{[\text{Ca}^{2+}]_{\text{sw}} \times [\text{CO}_3^{2-}]_{\text{sw}}}{K_{\text{sp}}} \quad (7)$$

81

82 where $[\text{Ca}^{2+}]_{\text{sw}}$ and $[\text{CO}_3^{2-}]_{\text{sw}}$ are calcium ion (Ca^{2+}) and CO_3^{2-} concentration in seawater and K_{sp} is the
83 empirically determined solubility product (Mucci, 1983). K_{sp} differs for different crystal forms of CaCO_3 . It is
84 higher for Aragonite than for Calcite, meaning Aragonite is more soluble (Mucci, 1983). Aragonite (Ara) and
85 Calcite (Cal) precipitation is thermodynamically favoured when Ω_{Ara} and Ω_{Cal} are ≥ 1 . CaCO_3 precipitation is of
86 high relevance for the assessment of OAE as the drawdown of CO_3^{2-} through precipitation reduces alkalinity,
87 shifts the carbonate chemistry equilibrium (eq. 1) towards CO_2 and thus counters the CDR efficiency of OAE
88 (Fuhr et al., 2022; Hartmann et al., 2023; Moras et al., 2022).

89 Logistical constraints suggest that OAE would at least initially more likely to be conducted in coastal
90 environments (He and Tyka, 2023; Lezaun, 2021; Renforth and Henderson, 2017). Here, alkalinity-enhanced
91 seawater would likely be in contact with marine sediments (Feng et al., 2017; Harvey, 2008; Meysman and
92 Montserrat, 2017). The highly abundant particles in marine sediments can serve as nuclei for CaCO_3 precipitation
93 thereby catalysing alkalinity loss when Ω_{CaCO_3} is ≥ 1 (Morse et al., 2003; Zhong and Mucci, 1989). This constitutes
94 a problem for OAE because alkalinity-enhanced seawater with its high Ω_{CaCO_3} is then exposed to particles that
95 catalyse precipitation. Indeed, recent studies have demonstrated that this particle-catalysed precipitation can
96 rapidly reduce alkalinity, with the degree and rate of alkalinity reduction depending on the amount of alkalinity
97 added and the particle concentrations (Fuhr et al., 2022; Hartmann et al., 2023; Moras et al., 2022).

98 Particle-catalysed CaCO_3 precipitation has received significant consideration as a loss term for OAE efficiency
99 (Fuhr et al., 2022; Hartmann et al., 2013, 2023; Moras et al., 2022; Renforth and Henderson, 2017). However,
100 there is another complication associated with OAE near sediments, which has to the best of my knowledge not
101 been considered so far. Sediments can not only provide precipitation nuclei but also constitute natural alkalinity
102 sources, for example via dissolution of CaCO_3 or other carbonates.

103 Sandy beaches are often rich in biogenic carbonates. They can also be rich in organic matter thereby
104 creating environments of high respiratory CO_2 . Accordingly, Ω_{CaCO_3} is low close to the sediments or within pore
105 waters and CaCO_3 dissolution is favoured (Liu et al., 2021; Perkins et al., 2022; Reckhardt et al., 2015). This form
106 of natural alkalinity formation via CaCO_3 dissolution sequesters respired CO_2 which may have otherwise be
107 released into the atmosphere (Aller, 1982; Fakhraee et al., 2023; Krumins et al., 2013; Saderne et al., 2021). OAE
108 within these naturally low Ω_{CaCO_3} environments could have two effects. First, it would have the desired effect of
109 consuming H^+ and increasing CO_2 sequestration via the generation of anthropogenic alkalinity (eqs. 2-4). Second,
110 the consumption of H^+ would increase Ω_{CaCO_3} , which could reduce the dissolution of CaCO_3 and thus reduce
111 natural CO_2 sequestration since less natural alkalinity is produced. Due to this second effect, the first (desired)
112 effect of CO_2 sequestration may be significantly reduced. Accordingly, the net gain in CO_2 sequestration would
113 be lower than one would have hoped for.

114 The concept “additionality” describes the net gain in CO_2 sequestration achieved through the
115 implementation of a CDR method. It can be defined in simple terms as:

116

117
$$\text{Additionality} = C_{\text{OAE}} - \Delta C_{\text{baseline}} \quad (8)$$

118





119 where C_{OAE} is the CO_2 sequestration achieved through OAE, and $\Delta C_{baseline}$ is the change in the baseline CO_2
120 sequestration through the implementation of OAE.

121 This study aims to reveal and describe how anthropogenic alkalinity affects natural alkalinity release. I
122 present some observational data and three experiments where 3 types of anthropogenic alkalinity sources (NaOH,
123 steel slag, olivine) are exposed to a natural alkalinity source and sink (beach sand) to investigate their interactions.
124 Afterwards, I examine these interactions (termed “additionality problem”), discuss their relevance, and how it
125 could be mitigated.

126

127 2. Methods

128

129 2.1. Carbonate chemistry and dissolved silicate transects along Southern Tasmanian beaches

130

131 The project was initialised with near-shore alkalinity, pH, and dissolved silicate (DSi) transects from the swash
132 zone to ~200 m offshore on 4 beach locations (Clifton South, Clifton North, Goats, Wedge) near Hobart
133 (Tasmania). Goal of these transects was to determine whether the beaches are detectable alkalinity sinks or sources
134 and to inform the incubation experiments. An overview of the sampled beaches with approximate conditions and
135 exact coordinates is provided in Table S1 and Fig. S1.

136 Samples for alkalinity and DSi were taken by filling 200 mL seawater from 0.2 m depth into a
137 polyethylene (PE) bottle. Samples for pH were collected in a 60 mL polystyrene (PS) jars filled and closed at 0.2
138 m depth. Both the PE bottles and the PS jars were pre-rinsed with sample. The sample closest to shore was taken
139 in the swash zone at the spot where a wave reached highest within ~5 minutes of observation. A ~0.2 m deep hole
140 was dug (Fig. S1) and water was collected from the groundwater with a 60 mL syringe. The second sample was
141 from the upper part of the swash zone where waves pushed water up the beach. Samples further out were taken
142 from within the wave breaking zone to about 50-100 m beyond the wave breaking zone. Samples were taken by
143 walking into the water to the point it became too deep and a surfboard was used as sampling vehicle.

144 The samples were transported back to the beach where pH was measured immediately (i.e. within 15
145 minutes after sampling) as described in section 2.4. Alkalinity and DSi samples were filtered after pH
146 measurements with a 0.22 syringe filter (nylon membrane) into a 125 mL PE bottle (alkalinity) or 60 mL PS
147 plastic jar (DSi). Both containers, the syringe, and the syringe filter were pre-rinsed with sample.

148

149 2.2. Laboratory experiments

150

151 2.2.1. Experiment 1: Replicated mineral dissolution assays to monitor interaction between 152 beach sand and weathering minerals

153

154 Experiment 1 was designed to investigate the interaction between 4 different beach sands and alkaline minerals
155 during the incubation in seawater. The experiment required 60 HDPE bottles, each with a volume of 125 mL.
156 These 60 bottles were thoroughly cleaned with double-deionised water and dried at 60°C. Twelve bottles were
157 filled with sand from one of the 4 sampling locations (section 2.3.), respectively (totalling 48 bottles). Another
158 set of 12 bottles were not filled with sand. This yielded 5 sets of 12 bottles (Fig. 1). Of each set, 3 bottles remained



159 without further addition, 3 received 51.3 μL of 1 molar NaOH, 3 received 0.0065 g of ground steel slag, and 3
160 received 1 g of ground olivine (Fig. 1; sand, steel slag, and olivine properties were determined as described in
161 section 2.3.). The 48 bottles that contained sand were filled with 10 g of sand if slag or NaOH was added or 9 g
162 of sand if olivine was added. This was done so that the weights of added sand plus alkalinity feedstock was always
163 ~ 10 g.

164 Once the solid components were added, each bottle was filled with 120 (+/-4) g of seawater ($S=35 \pm 2$, alkalinity
165 = 2259.7 $\mu\text{mol/kg}$) collected in July 2022 in the Derwent Estuary near Taroona. Salinity and pH of the seawater
166 was determined a few minutes before transfer into the incubation bottles with a Metrohm 914 pH/conductivity
167 meter as described in section 2.4. The transfer of the seawater into the incubation bottles took 30 minutes in total
168 (please note that in the case of NaOH additions, seawater was added to the bottles before 51.3 μL of 1 molar
169 NaOH was added). The incubation bottles were immediately mounted on plankton wheel (1.06 m diameter, 2
170 rounds per minute), which was placed in a temperature-controlled room set to 15°C (Fig. S2). The plankton wheel
171 kept the various mixtures of sand, alkalinity source, and seawater moving inside the bottles. The experiment
172 commenced at 16:00 on the 17th of August, 2022.

173 After ~ 6.8 days (24th of August), bottles were consecutively removed from the plankton wheel in random order
174 between 8:00 and 15:30. pH was measured inside the bottle with a pH electrode, directly after a bottle was taken
175 off the plankton wheel. Afterwards, the alkalinity sample was filtered with a syringe through a 0.2 μm nylon filter
176 into a dry and clean 125 mL HDPE bottle and stored in the dark at 7°C.

177

178 2.2.2. Experiment 2: Alkalinity formation at Omega gradients

179

180 Experiment 2 was designed to investigate whether a decline of Ω_{CaCO_3} enhances the formation of natural alkalinity
181 via CaCO_3 dissolution and how anthropogenic alkalinity sources (olivine, slag, NaOH) influence this process. The
182 experiment required 60 HDPE bottles (125 mL) cleaned with acid and double-deionised water (note that acid was
183 used in Experiment 2 to make sure all remnants from Experiment 1 were washed out of the bottles). All 60
184 incubation bottles were filled with sand from Clifton Beach (section 2.4.). The treatments were then set up as
185 follows: Twelve bottles were filled only with 10 g of sand; Twelve with 10 g of sand and 0.006515 (+/-0.00007)
186 g steel slag; Twelve with 9 g of sand and 1 (+/-0.002) g of olivine; Eight with 10 g of sand at “un-equilibrated”
187 NaOH addition; Sixteen with 10 g of sand at “equilibrated” NaOH addition (Fig. 1).

188 For each treatment, a gradient in seawater CO_2 concentrations was established from bottle 1 (lowest CO_2) to bottle
189 8-16 (highest CO_2). This was achieved with the following approach: A batch of seawater ($S= 35 \pm 0.2$, alkalinity =
190 2266.8 $\mu\text{mol/kg}$) was collected in November 2022 in the Derwent Estuary near Taroona. About 0.3L of the batch
191 was bubbled with pure CO_2 gas for about 5 minutes to generate highly CO_2 -enriched seawater. Another $\sim 7\text{L}$ of
192 the batch was used as source water to fill the incubation bottles. pH and temperature were measured in this batch
193 prior to filling the incubation bottles. The low CO_2 incubation bottles (bottle 1 in the sequence from e.g. 1 to 12,
194 Fig. 1) were then filled first. Afterwards, about 20 mL of the CO_2 -enriched water was added to the batch, shaken
195 thoroughly to mix it and the pH and temperature were measured again. Once a stable pH/temperature reading was
196 achieved, the next bottles (bottle 2) were filled. This procedure was repeated until all bottles in a treatment were
197 filled with an increasing CO_2 concentration. For the equilibrated and un-equilibrated NaOH treatments, I followed
198 the same procedure but separate 0.3L and 7L batches were used for the CO_2 enrichment that had previously been



199 amended with NaOH to elevate alkalinity from 2266.8 to 2757.4 $\mu\text{mol/kg}$ prior to filling the incubation bottles.
200 All 60 bottles were filled with 120 \pm 4 g of seawater and immediately mounted on the plankton wheel (2nd of
201 December, 2022; 17:00) under the same conditions as in Experiment 1 (i.e. 15°C, 2 rounds per minute, Fig. S2).
202 After \sim 6.8 days (9th of December), bottles were removed from the plankton wheel between 9:00 and 16:00. pH
203 and alkalinity were sampled as described in section 2.2.1.

204

205 2.2.3. Experiment 3: pH dependency of alkalinity formation from slag and olivine

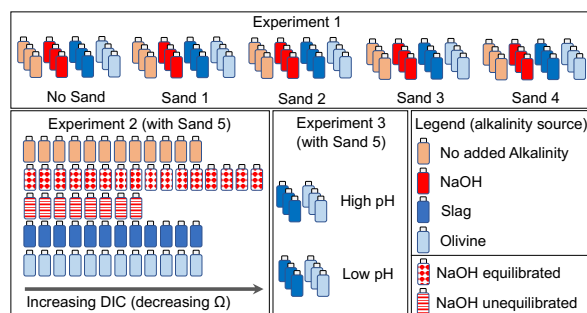
206

207 Experiment 3 was designed to investigate whether a lower seawater pH would promote alkalinity formation from
208 steel slag and olivine.

209 The experiment required 12 new HDPE bottles (125 mL) cleaned with double-deionised water and dried
210 thereafter. Six of the 12 bottles were filled with 0.00644 (\pm 0.00007) g steel slag and the other six with 1.0003
211 (\pm 0.002) g of olivine. Three slag and three olivine bottles were filled with seawater from the same seawater source
212 as used in Experiment 2 ($S=35\pm 0.2$, alkalinity=2263.2 $\mu\text{mol/kg}$, $\text{pH}_T = 7.82$). pH and temperature were measured
213 prior to filling the bottles with seawater (section 2.4.). Afterwards, the \sim 2L seawater batch was amended with
214 about 80 mL of CO_2 -enriched seawater as explained in section 2.2.2. This enrichment lowered the pH_T (total
215 scale) from 7.82 to 6.846. This low pH_T (high CO_2) seawater was used to fill the other 3 slag and olivine incubation
216 bottles. The 12 bottles with 122.8 (\pm 0.15) g of seawater were immediately mounted on the plankton wheel (Fig.
217 S2) after filling (16th of December, 2022; 16:40) under the same conditions as in Experiment 1 and 2 (i.e. 15°C,
218 2 rounds per minute).

219 After \sim 6.8 days (23rd of December), the 12 bottles were randomly removed from the plankton wheel between 9:00
220 and 11:00. pH and alkalinity were sampled as described in section 2.2.1.

221



222

223 **Figure 1.** Design of Experiments 1, 2, and 3. Bottles represent treatments with incubation of seawater, sand, and
224 alkalinity sources (color code represents alkalinity source). In Experiment 2, NaOH was used as alkalinity source
225 in two explicit scenarios as described in section 2.2.2.

226

227 2.3. Preparation and characterization of weathering minerals and beach sand

228

229 In total, 5 sand samples (0.5-1kg) were collected for Experiments 1 and 2 at Clifton Beach, Tasmania (Fig. S1,
230 Table S1). Sampling permission was granted by the Department of Natural Resources and Environment (Authority
231 No. ES 22314). Wet sand was sampled on the upper end of the swash zone and stored in zip bags at 15°C. Samples



232 1-4 were used for Experiment 1, ~24 hours after sampling while sample 5 was used for Experiment 2, ~72 hours
233 after sampling.

234 Olivine rocks were sourced from the Mount Shadwell Quarry in Mortlake (Australia, Table S1). Basic oxygen
235 slag (hereafter just called slag) was sourced from the Liberty Primary Steel – Whyalla Steelworks (Australia,
236 Table S1). Olivine rocks and slag (Fig. S3) were crushed with a hydraulic crusher into smaller pieces of about 10
237 mm and then milled with a ring mill in a chrome milling pot. Milled slag and olivine were sieved, first with a 250
238 μm sieve and then with a 150 μm sieve. The fractions retained on the 150 μm sieve were used for experiments.

239 Wet and dry weight of the sand used for laboratory experiments was determined by weight difference of a wet
240 and a dry sample. The wet sample (~80 g) was put into a clean plastic jar and dried for 24-72 hours. The particle
241 size spectra of the 5 dried sand samples as well as slag and olivine mineral were determined with a Sympatec
242 QICPIC particle imager.

243 For total particulate carbon (TPC) and particulate organic carbon (POC) analyses, dried sand samples were milled
244 for 12 minutes in a Retsch MM200 ball mill. Between 4-10 mg of each of the pulverized sand samples were
245 weighed into 10 tin cups for TPC or 10 silver cups for POC (2 TPC and POC replicates for each sample). The
246 POC samples were moisturized with 50 μL of MilliQ water, placed for 18 hours in a dessicator that contained 36%
247 HCl to remove all carbonates and then dried. TPC and POC samples were analysed for carbon content using a
248 Thermo Finnigan EA 1112 Series Flash Elemental Analyser. Particulate inorganic carbon (PIC) content of the
249 samples was then calculated as the difference between TPC and POC. Percent content of carbonates was estimated
250 by multiplying % PIC content by the molecular weight of CaCO_3 (100 g/mol) and MgCO_3 (84.3 g/mol) for upper
251 and lower estimates.

252

253 **2.4. Carbonate chemistry, salinity, and dissolved silicate measurements**

254

255 pH was determined potentiometrically using a Metrohm 914 pH meter following Standard Operation Procedure
256 6a described in (Dickson et al., 2007) but omitting the test for ideal Nernst behaviour of the electrode (ideal Nernst
257 behaviour was assumed). A new pH electrode (Metrohm Aquatrode Plus) was calibrated on the total pH scale
258 (pH_T) with certified reference material (CRM) TRIS buffer (batch #37), provided by Prof. Andrew Dickson's
259 laboratory. The calibration procedure for the relevant temperature range (~8 – 18°C) followed the exact workflow
260 as described by (Ferderer et al., 2022). Precision of the pH measurement was assumed to be ± 0.015 based on
261 experience with the probe.

262 alkalinity was determined in an open cell titration following (Dickson et al., 2003). Samples were measured in
263 duplicate with a Metrohm 811 titration unit equipped with a Metrohm Aquatrode Plus. Alkalinity was calculated
264 from titration curves using the Calculate function of PyCO2sys (Humphreys et al., 2020). The difference in
265 alkalinity between duplicate titrations of the sample was on average 1.95 $\mu\text{mol}/\text{kg}$ and >75% were within 4
266 $\mu\text{mol}/\text{kg}$ (N=185), which was assumed to be the precision of the measurement ($\pm 2 \mu\text{mol}/\text{kg}$). Accuracy was
267 controlled by correcting alkalinity values with CRM provided by A.G. Dickson's laboratory. Alkalinity was
268 measured within maximally 20 days after sampling.

269 Salinity was measured with a Metrohm conductivity probe with a PT1000 temperature sensor connected to a
270 Metrohm 914 conductivity meter. The probe was calibrated with DIC/alkalinity CRM from A.G. Dickson's
271 laboratory for which a salinity of 33.464 has been reported (CRM batch 200). Conductivity was measured in



272 mS/cm² and salinity was subsequently calculated on the practical salinity scale following Lewis and Perkins
273 (1978), following the workflow described by (Moras et al., 2022). A relatively low precision of +/- 0.2 was
274 determined from repeat measurements.

275 Si concentrations for beach transects were measured 18 hours after sampling following Hansen and Koroleff
276 (1999). No Si measurements were conducted for Experiments 1-3.

277

278 **2.5. Carbonate chemistry calculations**

279

280 Carbonate chemistry conditions were calculated with the “carb function” in Seacarb (Gattuso et al., 2021), with
281 pH_r, alkalinity, salinity, temperature, phosphate and silicate concentrations as input variables, stoichiometric
282 equilibrium constants from Lueker et al. (2000), and default settings for the other equilibrium constants. Si was
283 not measured due to volume limitations so I assumed a values of 50 μmol/kg at the end of the experiments, when
284 either sand, olivine, or slag were incubated. Likewise, phosphate was not measured and I assumed 2 μmol/kg at
285 the end of the experiments when slag was incubated. These Si and phosphate releases were based upon previous
286 trials. Note, however, that concentrations of Si and phosphate within these ranges have negligible impact on
287 calculated carbonate chemistry parameters (e.g. pCO₂ changes by ~1 μatm when Si is assumed to be 0 instead of
288 50 μmol/kg).

289 Propagated errors in derived carbonate chemistry parameters (e.g., DIC) were calculated with the
290 “errors” function in Seacarb using measurement precisions described in section 2.4. for pH (±0.015), alkalinity
291 (±2 μmol/kg), and salinity (±0.2), default uncertainties for equilibrium constants and temperature, and when
292 applicable (see above) ±50 μmol/kg for silicate and ±2 μmol/kg for phosphate.

293

294 **2.6. Calculations of the CO₂ uptake ratio (η_{CO2}) for carbonate and non-carbonate alkalinity** 295 **sources**

296

297 The atmospheric CO₂ uptake ratio for OAE (η_{CO2}) was defined as the number of moles DIC absorbed per number
298 of moles alkalinity added (Tyka et al., 2022). η_{CO2} was shown to range roughly between 0.75 and 0.9 mol:mol in
299 the surface ocean (Schulz et al., 2023; Tyka et al., 2022). However, this η_{CO2} range only applies for alkalinity
300 source materials that exclusively increase alkalinity without a concomitant increase in DIC when they are added
301 to seawater (Alk_{non-carbonate}). Such sources comprise for example NaOH, slag, and olivine. The estimated range
302 does not apply when all or fractions of the added alkalinity comes from carbonates (Alk_{carbonate}), since CaCO₃
303 dissolution contributes 2 moles of alkalinity and 1 mole of (non-atmospheric) DIC when they dissolve.

304 The dependency of η_{CO2} on the relative contribution of Alk_{carbonate} and Alk_{non-carbonate} was calculated as:

305

$$306 \eta_{CO_2} = \frac{DIC_{equilibrated} - \left(\frac{Alk_{carbonate}}{2}\right) - DIC_{initial}}{Alk_{non-carbonate} + Alk_{carbonate} - Alk_{initial}} \quad (9)$$

307

308 Where DIC_{initial} and Alk_{initial} are DIC and alkalinity in seawater before alkalinity was increased, assuming a
309 seawater pCO₂ in equilibration with the atmosphere. DIC_{equilibrated} is the amount of DIC from the environment (e.g.
310 from the atmosphere) that can be stored in seawater after the increase of Alk_{carbonate} and Alk_{non-carbonate}, assuming




311 seawater $p\text{CO}_2$ in equilibrium with the atmosphere. η_{CO_2} was first calculated for a theoretical case where $\text{Alk}_{\text{initial}}$
312 was $2350 \mu\text{mol/kg}$ and $\text{DIC}_{\text{initial}}$ was calculated for the surface ocean (15°C , $S = 35$, carbonate chemistry constants
313 as in section 2.5), assuming a $p\text{CO}_2$ of $420 \mu\text{atm}$. $\text{Alk}_{\text{carbonate}}$ and $\text{Alk}_{\text{non-carbonate}}$ were then varied in a range of
314 scenarios (from 0 to 100% $\text{Alk}_{\text{carbonate}}$) to increase the sum of them by $1 \mu\text{mol/kg}$. η_{CO_2} was calculated for each
315 scenario.

316 Next, η_{CO_2} was calculated specifically for Experiment 1 as follows: The increase of alkalinity ($\Delta\text{Alkalinity}$) was
317 higher in the NaOH and slag treatments when no sand was present compared to incubations with sand (section
318 3.2). $\Delta\text{Alkalinity}$ was very likely $\text{Alk}_{\text{non-carbonate}}$ in all incubations while the reduced $\Delta\text{Alkalinity}$ in the incubations
319 with sand was likely due to secondary precipitation of carbonates (section 4.2.1). Based on these conclusions,
320 η_{CO_2} was estimated as:

321

$$322 \eta_{\text{CO}_2} = \frac{(\Delta\text{Alkalinity}_{\text{no-sand}} - \Delta\text{Alkalinity}_{\text{sand}}) \times 0.5 + \Delta\text{Alkalinity}_{\text{sand}} \times 0.86}{\Delta\text{Alkalinity}_{\text{no-sand}}} \quad (10)$$

323  where $\Delta\text{Alkalinity}_{\text{no-sand}}$ and $\Delta\text{Alkalinity}_{\text{sand}}$ are the changes in alkalinity measured in incubations without sand and
324 with sand, respectively; 0.5 is the η_{CO_2} when $\text{Alk}_{\text{non-carbonate}}$ is lost via the precipitation of carbonates where 2 moles
325 of alkalinity and 1 mol of DIC are sequestered; 0.86 is the η_{CO_2} when all $\Delta\text{Alkalinity}$ is $\text{Alk}_{\text{non-carbonate}}$ under the
326 conditions set up in the experiments (i.e. 15°C , $S=35$; see above). Please note that $\Delta\text{Alkalinity}$ was higher in the
327 olivine incubations when sand was present, which is opposite to the NaOH and slag incubations for reasons
328 discussed in section 4.2.1. Therefore, η_{CO_2} was calculated assuming all $\Delta\text{Alkalinity}$ was $\text{Alk}_{\text{non-carbonate}}$ for the
329 olivine incubations (i.e. $\eta_{\text{CO}_2} = 0.86$). For the incubations without an added alkalinity source all $\Delta\text{Alkalinity}$ was
330 assumed to be $\text{Alk}_{\text{carbonate}}$ so that η_{CO_2} was 0.36.

331 η_{CO_2} was also specifically calculated for Experiment 2. This required knowledge of how much of the measured
332 $\Delta\text{Alkalinity}$ was contributed by $\text{Alk}_{\text{carbonate}}$ and $\text{Alk}_{\text{non-carbonate}}$. In the treatments where only sand was incubated,
333 alkalinity and DIC increased roughly in a 2:1 molar ratio over the course of the experiment (i.e. $\Delta\text{Alkalinity}:\Delta\text{DIC}$
334 = 2:1 mol:mol). Thus, it can be assumed that the vast majority of the measured alkalinity increase is $\text{Alk}_{\text{carbonate}}$.
335 In contrast, when sand was incubated with alkaline materials, alkalinity and DIC generally increased with a molar
336 ratio that was $>2:1$ because alkaline materials release alkalinity without a concomitant increase of DIC. Based on
337 these constraints, we can roughly approximate the contribution of $\text{Alk}_{\text{carbonate}}$ and $\text{Alk}_{\text{non-carbonate}}$ to the measured
338 alkalinity increase ($\Delta\text{Alkalinity}$) as:

339

340

$$341 \% \text{Alk}_{\text{carbonate}} = \left(\frac{\Delta\text{Alkalinity}}{\Delta\text{DIC}} \right) / 2 \times 100 \quad (11)$$

342

343 Where $\% \text{Alk}_{\text{carbonate}}$ is the percentage contribution of $\text{Alk}_{\text{carbonate}}$ to $\Delta\text{Alkalinity}$. Based on eq. (11), a
344 $\Delta\text{Alkalinity}:\Delta\text{DIC}$ of for example 8:1 mol:mol would suggest that 25% of the $\Delta\text{Alkalinity}$ is $\text{Alk}_{\text{carbonate}}$ and the
345 other 75% $\text{Alk}_{\text{non-carbonate}}$. $\text{Alk}_{\text{carbonate}}$ and $\text{Alk}_{\text{non-carbonate}}$ were calculated with eq. 11 for all incubations in Experiment
346 2 and this information was then used to calculate η_{CO_2} with eq. (10). Finally, the amount of DIC that can be stored
347 in seawater due to an increase of $\text{Alk}_{\text{carbonate}}$ and $\text{Alk}_{\text{non-carbonate}}$ (DIC_{OAE}) was calculated as:

348



349 $DIC_{OAE} = \eta_{CO_2} * \Delta\text{Alkalinity}$ (12)

350

351 for experiments 1 and 2.

352

353 2.7. Statistical analysis

354

355 Experiment 1 and 3 were analysed with a two-way analysis of variance (ANOVA) where either “sand” and
356 “alkalinity source material” (Experiment 1) or “carbonate chemistry” and “alkalinity source material”
357 (Experiment 3) were defined as independent variables. The dependent variables were the changes in carbonate
358 chemistry (e.g. $\Delta\text{Alkalinity}$) over the course of the incubations. Homogeneity of variance was assessed by visually
359 inspecting if plotted model residuals vs. fitted values is scattering similarly around 0. Normality of the residuals
360 was assessed by inspecting qqplots where theoretical quantiles plotted against standardized residuals should
361 ideally resemble a straight line. Such a straight-line appearance (i.e. ideal normality) was not always given, so
362 some datasets were rank-transformed. However, transformation did not improve normality substantially so that
363 non-transformed data was used for all analyses. Statistical differences between individual treatments were
364 assessed with a Tukey post-hoc. Significant differences were assumed when $p < 0.05$.

365 Experiment 2 was analysed by plotting $\Delta\text{Alkalinity}$ for each alkalinity source material and sand against the
366 increase in DIC that was established via additions of CO_2 -saturated seawater (section 2.2.2). The data was fitted
367 with the polynomial equation $a*x^2+bx+c$, where x is the amount of DIC added to each treatment and a , b , c are
368 fit parameters. The curve fitted to the treatments where only sand was added was compared to the curves fitted to
369 the treatments where sand and a certain alkalinity source were added.

370

371 3. Results

372

373 3.1. Beach transects

374

375 Beach transects consisted of 8-9 sampling points from the just above the swash zone to 150-220 m offshore at
376 four locations (Table S1, Fig. S1). Alkalinity showed distinct patterns across the locations. At Clifton South and
377 Wedge, alkalinity was higher in the swash zone than in the open water. This was particularly pronounced at Clifton
378 South with a value of 2418 $\mu\text{mol/kg}$ relative to open water values of about 2300 $\mu\text{mol/kg}$ (Fig. 2A). At Goats
379 Beach, no such alkalinity gradient was observed across the transect, while alkalinity was lower in the swash zone
380 at Clifton North (Fig. 2A). Wedge differed to the other locations in that alkalinity was generally lower (~2160
381 compared to ~2300 $\mu\text{mol/kg}$ in open water).

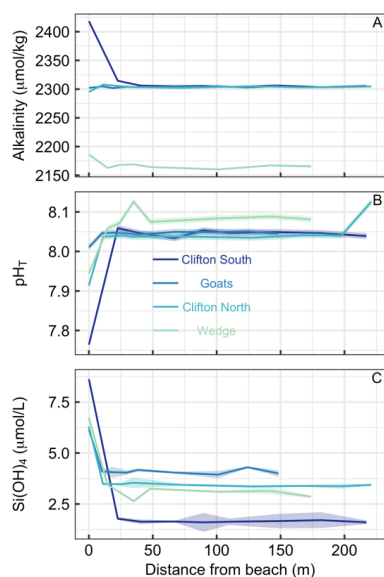
382 pH_T was lowest in samples just above the swash zone at all four locations (Fig. 2B). The difference relative to
383 open water was most pronounced at Clifton South with pH_T of 7.76 just above the swash zone compared to
384 approximately 8.05 in the open water, while least pronounced at Goats. Gradients at Clifton North and Wedge
385 were in between these two extremes. pH_T at Wedge was on average higher in the open water than at the other
386 locations, i.e. 8.08 compared to 8.05 (Fig. 2B).

387 $\text{Si}(\text{OH})_4$ concentrations were highest in samples from just above the swash zone at all four locations (Fig. 2C).

388 The most pronounced gradient was observed at Clifton South, with $\text{Si}(\text{OH})_4$ of 8.6 $\mu\text{mol/L}$ just above the swash



389 zone and $\sim 1.6 \mu\text{mol/L}$ in open water. The least pronounced gradient was observed at Goats, and intermediate
390 gradients at Clifton North and Wedge (Fig. 2C).
391 Overall, the data shows consistency across the three parameters measured in that Clifton South showed most
392 pronounced trends, Goats the least pronounced trends, and Clifton North and Wedge being in between (Fig. 2).



393
394 **Figure 2.** Transects of (A) alkalinity, (B) pH_T , and (C) Si(OH)_4 at four different beach locations in southern
395 Tasmania (see Table S1 and Fig. S1 for locations). The first sampling was at the upper end of the swash zone and
396 then 7-8 more samples were taken until 150-200 m offshore. Lines and shaded areas show averages and
397 uncertainties, respectively.

398

399

3.2. Experiment 1

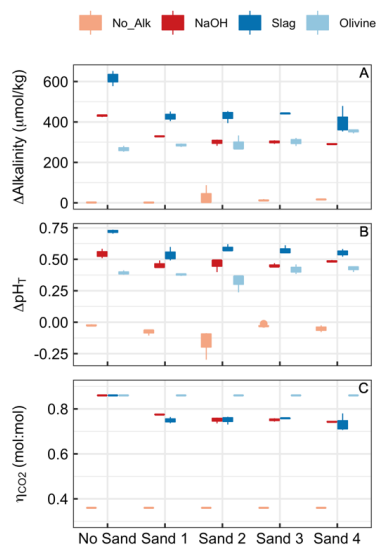
400

401 Alkalinity increased over the course of the 6.8 days in all treatments where alkaline materials were added (Fig.
402 3). Changes in alkalinity ($\Delta\text{Alkalinity}$) were between $\sim 610\text{--}400 \mu\text{mol/kg}$ for the slag, $\sim 420\text{--}290 \mu\text{mol/kg}$ for the
403 NaOH, and $280\text{--}370 \mu\text{mol/kg}$ for the olivine treatment. In contrast, $\Delta\text{Alkalinity}$ changed very little (i.e. $\Delta\text{Alkalinity}$
404 $\leq 6 \mu\text{mol/kg}$) when no alkaline materials were added. (Please note that an important outlier was observed in Sand
405 2 where $\Delta\text{Alkalinity}$ was $87.3 \mu\text{mol/kg}$ which will be discussed in section 4.3.). The two-way ANOVA revealed
406 significant effects of (1) the type of sand, (2) the type of alkalinity source, and (3) the interaction of these two on
407 $\Delta\text{Alkalinity}$ ($p < 0.05$). For the slag and the NaOH treatment, $\Delta\text{Alkalinity}$ was significantly higher when these were
408 incubated with no sand but only small differences were observed across the four sand samples. In contrast,
409 $\Delta\text{Alkalinity}$ was slightly lower in the olivine treatment when no sand was present during incubations although the
410 difference was only significant relative to olivine incubated in Sand 4 (Fig. 3A).

411 Changes in pH_T (ΔpH_T) reflected the patterns described for $\Delta\text{Alkalinity}$ (Fig. 3B). ΔpH_T was highest in the slag
412 and the NaOH treatment when no sand was added, while this difference between the presence and absence of sand
413 was not observed for olivine. ΔpH_T was slightly negative in treatments where no alkalinity source was added to



414 the incubated sand samples. The two-way ANOVA revealed significant effects of sand, alkalinity source and their
415 interaction on ΔpH_T ($p < 0.05$).
416 η_{CO_2} was prescribed to be 0.36 when sand without an anthropogenic alkalinity source was incubated and 0.86 for
417 olivine incubations (see section 2.6). Calculated η_{CO_2} for NaOH and slag treatments were slightly lower due to
418 relatively lower $\Delta\text{Alkalinity}$ in the presence of sand than without the presence of sand (Fig 3C). This relatively
419 lower $\Delta\text{Alkalinity}$ was most likely due to some of the $\Delta\text{Alkalinity}$ was lost due to secondary precipitation of
420 carbonates. Statistics are not provided for η_{CO_2} data because assumptions of the ANOVA model were heavily
421 violated.
422



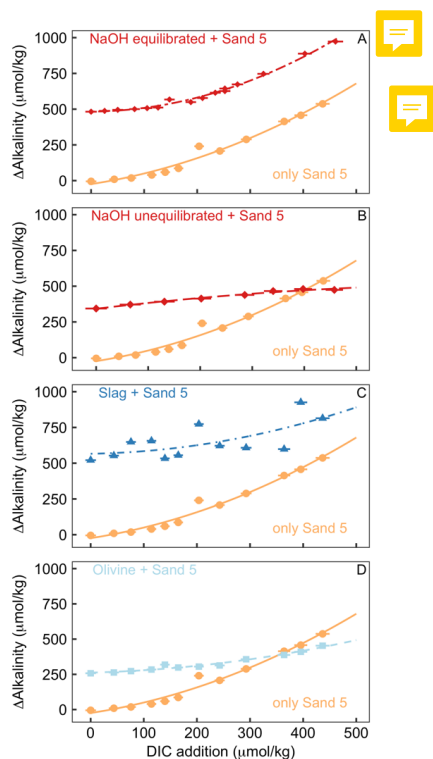
423
424 **Figure 3.** Results of Experiment 1. Changes of (A) alkalinity and (B) pH_T from the beginning to the end of the
425 6.8 days experiment. (C) η_{CO_2} at the end of the experiment. Boxplots are based on three replicates per treatment.
426 Colours refer to the added alkalinity source (No_Alk means no alkalinity source was added). The alignment on
427 the x-Axis indicates if or which sand sample was present in the incubation bottles (“No Sand” means no Sand was
428 added).

430 3.3. Experiment 2

431
432 The additions of CO_2 -enriched seawater established a gradient of increasing DIC and accordingly a decline in
433 pH_T and Ω_{Ara} . The rationale for this setup was that beach sediments can contain high amounts of respiratory CO_2
434 so that anthropogenic alkalinity added to beaches has a high likelihood to be exposed to such high CO_2 conditions
435 (Liu et al., 2021; Perkins et al., 2022; Reckhardt et al., 2015). Fig. 4 shows $\Delta\text{Alkalinity}$ along the DIC gradient
436 for different alkalinity source materials (NaOH, slag, olivine) and compares this to $\Delta\text{Alkalinity}$ along the same
437 DIC gradient where only sand from a beach was present. The “sand only” data is identical in all four plots (orange
438 lines in Fig. 4). It shows that $\Delta\text{Alkalinity}$ is close to zero in the sand-only incubations when no DIC is added but
439 increases exponentially with increasing DIC additions up to $537 \mu\text{mol/kg}$.



440 OAE via NaOH additions was set up in two different scenarios (Fig. 4A, B). In the first scenario, the carbonate
441 system was equilibrated with atmospheric CO₂ after the NaOH deployment and before exposed to the sand (Fig.
442 4A). This setup leads to a gradient in $\Omega_{\text{Ar}}^{\text{Ar}}$ from 2.1 to 0.2 along the DIC gradient at the beginning of the 6.8 days
443 incubations (highest $\Omega_{\text{Ar}}^{\text{Ar}}$ at the lowest DIC addition). In the second scenario, the carbonate system was not
444 equilibrated, thereby assuming that a NaOH-enriched patch of seawater would be exposed to sand sediments
445 before it had taken up atmospheric CO₂ (Fig. 4B). Here, initial $\Omega_{\text{Ar}}^{\text{Ar}}$ ranges from 7.1 to 2.3 along the DIC gradient.
446 In the equilibrated scenario, $\Delta\text{Alkalinity}$ was 482 $\mu\text{mol/kg}$ when no DIC was added and increased exponentially
447 to 973 $\mu\text{mol/kg}$ at the highest DIC addition (Fig. 4A). In the unequilibrated scenario, $\Delta\text{Alkalinity}$ was 344 $\mu\text{mol/kg}$
448 when no DIC was added and increased to 474 $\mu\text{mol/kg}$ at the highest DIC addition. However, in contrast to the
449 equilibrated treatment, the $\Delta\text{Alkalinity}$ increase weakened along the DIC gradient and $\Delta\text{Alkalinity}$ was lower than
450 in the sand-only treatment when the DIC addition was $>400 \mu\text{mol/kg}$ (Fig. 4B).
451 In the slag treatment, $\Delta\text{Alkalinity}$ was 521 $\mu\text{mol/kg}$ when no DIC was added. $\Delta\text{Alkalinity}$ increased exponentially
452 along the DIC gradient to 814 $\mu\text{mol/kg}$. The increase of $\Delta\text{Alkalinity}$ was less pronounced than in the sand-only
453 treatment. Overall, the slag data showed more scatter relative to the other alkalinity source materials and sand-
454 only treatments (Fig. 4C).
455 In the olivine treatment, $\Delta\text{Alkalinity}$ was 258 $\mu\text{mol/kg}$ when no DIC was added. $\Delta\text{Alkalinity}$ increased
456 exponentially with increasing DIC additions to 453 $\mu\text{mol/kg}$ although much less pronounced than in the sand-
457 only treatment. $\Delta\text{Alkalinity}$ was lower in the olivine than in the sand-only treatment when DIC additions were
458 $>350 \mu\text{mol/kg}$ (Fig. 4C).
459



460



461 **Figure 4.** Results of Experiment 2. All panels show the change in alkalinity from the beginning to the end of the
462 6.8 days experiment along a gradient of DIC added to the incubation bottles at the start of the incubations. The
463 orange data displayed on all panels show Δ Alkalinity for incubations where only sand was incubated. The other
464 data on each panel show Δ Alkalinity when sand was incubated with an external alkalinity source or addition
465 scenario. (A) Sand and NaOH equilibrated with atmospheric CO_2 upon addition; (B) Sand and NaOH which was
466 not equilibrated with atmospheric CO_2 upon addition; (C) Sand and slag; (D) Sand and olivine.

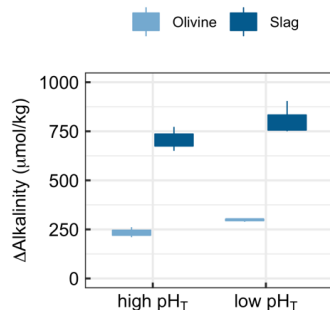
467

468 3.4. Experiment 3

469

470 Experiment 3 tested if there is a pH dependency of alkalinity release by olivine and slag (Fig. 5). The two-way
471 ANOVA revealed a significant influence of pH_T on the release of alkalinity from olivine and slag (Fig. 4). Slag
472 released $707 \pm 61 \mu\text{mol/kg}$ alkalinity when incubated within a pH_T from initially 7.82 to 8.67 at the end of the 6.8
473 days incubation. Within the lower pH_T range from 6.86-8.39, slag released $805 \pm 86 \mu\text{mol/kg}$. Olivine released
474 $234 \pm 36 \mu\text{mol/kg}$ within the high pH_T range from 7.82-8.20 and $298 \pm 8 \mu\text{mol/kg}$ in the low pH_T range from 6.86-
475 7.63 (Fig. 5).

476



477

478 **Figure 5.** Results of Experiment 3. Changes in alkalinity from the beginning to the end of the 6.8 days experiment
479 when olivine or slag were incubated (without sand) under high (initially 7.82) or low pH_T (initially 6.85).
480 Δ Alkalinity was significantly higher under low pH_T .

481

482 4. Discussion

483

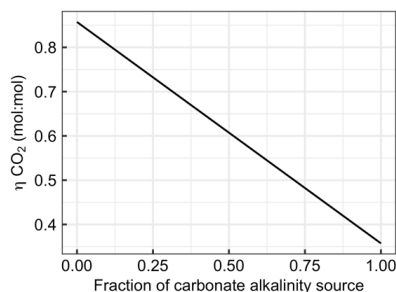
484 4.1. Carbonate-derived alkalinity is less efficient for CDR than non-carbonate-derived alkalinity

485

486 Section 2.6. introduced equations which show that alkalinity originating from carbonates ($\text{Alk}_{\text{carbonate}}$) has
487 considerably less capacity to absorb CO_2 than alkalinity originating from non-carbonate sources such as olivine,
488 slag, or NaOH ($\text{Alk}_{\text{non-carbonate}}$). The large influence of this chemical constraint on OAE is exemplified in Fig. 6.
489 Here, the uptake potential for atmospheric CO_2 per mol alkalinity added to the ocean (η_{CO_2}) is shown as a function
490 of the carbonate contribution to the alkalinity source. When all Δ Alkalinity delivered via OAE originates from
491 non-carbonate sources (e.g., NaOH, slag, olivine), then η_{CO_2} equals 0.86 mol:mol. η_{CO_2} declines linearly with an



492 increasing contribution $\text{Alk}_{\text{carbonate}}$ to $\Delta\text{Alkalinity}$ to the lowest theoretical value for η_{CO_2} of 0.36 mol:mol, which
493 is reached when OAE provides all alkalinity as $\text{Alk}_{\text{carbonate}}$ (Fig. 6).
494 The dependency of η_{CO_2} on the alkalinity source material (Fig. 6) has important implications for OAE methods
495 that aim to utilise CaCO_3 as alkalinity source (Harvey, 2008; Rau and Caldeira, 1999; Renforth et al., 2022;
496 Wallmann et al., 2022). The molar efficiency for atmospheric CO_2 sequestration of OAE is >50% lower when
497 using carbonates (e.g. CaCO_3). Or put differently, OAE approaches utilising CaCO_3 as alkalinity source would
498 have to increase alkalinity by more than twice as much to generate similar CDR compared to methods that use
499 non-carbonates (e.g. NaOH, slag, or olivine). Importantly, while this disadvantage of carbonates sources of
500 alkalinity appears to be substantial, it is not the only important factor determining the potential of such OAE
501 approaches. It is possible that the use of carbonates still holds higher potential, for example because limestone is
502 relatively abundant (Caserini et al., 2022), can dissolve (Renfort et al., 2022), or because it contains less
503 components potentially affecting marine organisms (Bach et al., 2019). Nevertheless, the dependency of η_{CO_2}
504 the alkalinity source (Fig. 6) needs to be considered when assessing the efficiency of different OAE methods, as
505 will become apparent in section 4.2.
506



507
508 **Figure 6.** Changes in η_{CO_2} with the fraction alkalinity that originates from carbonates (e.g. CaCO_3 dissolution).
509 The x-axis ranges from 0, which means all alkalinity originates from non-carbonate sources such as NaOH, slag,
510 or olivine to 1, which means all alkalinity originates from carbonate sources such as CaCO_3 or MgCO_3 .

511 512 4.2. The additionality problem of OAE

513
514 The experiments considered here investigate coastal applications of OAE, for example when ground minerals or
515 NaOH are exposed to beaches or sandy sediments. In the experiments, the treatments where only sand was
516 incubated constitute the baseline system while incubations of sand and an alkalinity source constitute the OAE
517 deployments. Both the baseline system and the OAE deployment were run in parallel under identical conditions.
518 To assess the net CO_2 sequestration (additionality) of OAE, CO_2 sequestration achieved through an OAE
519 deployment must be compared to the baseline state where no such deployment occurred (see eq. 8). As such,
520 additionality can be affected through processes that affect the OAE deployment directly (section 4.2.1.), or
521 through when the OAE deployment alters the baseline state of the system (section 4.2.2.).

522 523 4.2.1. Change of additionality through interaction of alkalinity sources with sand

524



525 The Δ Alkalinities determined in Experiment 1 were lower in NaOH and slag incubations with sand than in
526 incubations without sand. The reduction in the presence of sand was most likely due secondary precipitation of
527 carbonates, which is promoted when Ω_{CaCO_3} is elevated and particle abundance is high (Fuhr et al., 2022; Moras
528 et al., 2022; Zhong and Mucci, 1989). In the case of slag, very small amounts of particles were also present in the
529 incubation without sand but apparently not enough to catalyse a similar degree of secondary precipitation as in
530 the case when 10 g of sand are present.

531 In contrast to the NaOH and slag incubations, the olivine incubations generated more Δ Alkalinity when sand was
532 present, even though the enhancement was small and only in one case statistically significant (i.e. No Sand vs
533 Sand 4; Fig. 3A). This contrasting observation can be explained as follows. First, Δ Alkalinity was generally lower
534 in the olivine incubations than in the NaOH and slag incubations when no sand was present ($266 \pm 14.8 \mu\text{mol/kg}$
535 for olivine vs. $>420 \mu\text{mol/kg}$ for NaOH and slag). Moras et al. (2022) have shown that the onset of secondary
536 precipitation depends on Δ Alkalinity and they observed no secondary precipitation over a 40 days experimental
537 incubation when Δ Alkalinity was $\sim 250 \mu\text{mol/kg}$. This suggest that the $266 \pm 14.8 \mu\text{mol/kg}$ Δ Alkalinity generated
538 by olivine did not elevate Ω_{Ara} to high enough levels to induce noticeable secondary precipitation within 6.8 days.
539 However, the absence of such secondary precipitation cannot explain why Δ Alkalinity increased in the presence
540 of sand. It is possible that the sand itself released alkalinity via carbonate dissolution as a very small increase in
541 Δ Alkalinity was also observed in the sand-only incubations (e.g. $17.4 \pm 2.6 \mu\text{mol/kg}$ in Sand 4; Fig. 3A). However,
542 Ω_{Ara} was higher in the olivine incubations as in the sand-only treatment so that a release of carbonate alkalinity
543 seems unlikely. It is also unlikely that the pH differences between olivine-only and olivine+sand incubations
544 drove this trend. While Experiment 3 underscores that lower pH promotes the release of alkalinity from olivine
545 (Fig. 5), pHT was higher in the olivine+sand treatment where significantly more alkalinity was released (see Sand
546 4 in Fig. 4A). What appears as a plausible explanation is that the sand caused physical destruction of coatings that
547 develop on the olivine particles during dissolution and are known to reduce dissolution rates (Oelkers et al., 2018).
548 Indeed, the dissolution-enhancing role physical abrasion has been hypothesised to increase OAE efficiency when
549 using olivine, although the dataset underpinning this hypothesis has not made it through peer-review (Schuiling
550 and de Boer, 2011).

551 η_{CO_2} is reduced when the presence of sand catalyses secondary precipitation (Fig. 4C). As a consequence, the
552 amount of DIC that can be sequestered via OAE declines. Among other factors, the degree of alkalinity loss due
553 to secondary precipitation depends on the duration carbonate supersaturated water is exposed to the sand. The
554 experiments presented here lasted for 6.8 days and it is likely that secondary precipitation would have proceeded
555 (and η_{CO_2} further declined) if the experiments had lasted for longer. Indeed, Moras et al. (2022) observed that
556 secondary precipitation catalysed by particles only slowed down once Ω_{Ara} reached ~ 2 . In the experiments
557 presented here, Ω_{Ara} was generally >5 at the end of the study. Carbonate chemistry calculations with seacarb (data
558 not shown) suggest that a decline until Ω_{Ara} reaches 2 via carbonate precipitation (i.e. alkalinity and DIC decline
559 in a 2:1 molar ratio) would have reduced alkalinity by $\sim 560 \mu\text{mol/kg}$ for the NaOH and $840 \mu\text{mol/kg}$ for the slag
560 incubations, respectively. In both cases the alkalinity after the OAE perturbation would be lower than before but
561 atmospheric CO_2 uptake would still occur ($\eta_{\text{CO}_2} = 0.39$ for NaOH and 0.37 for slag) because the pCO_2 is still
562 slightly lower than before the perturbation (Moras et al., 2022).

563
564

4.2.2. Reduction of additionality through modification of baseline alkalinity formation



565

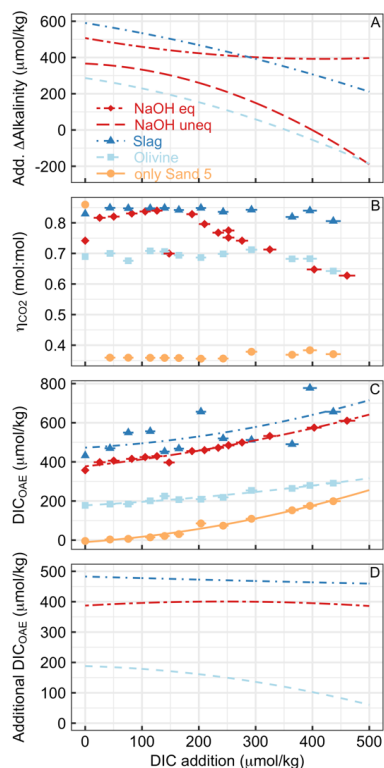
566 One interesting observation was made during a sand-only incubation of Experiment 1 (i.e. “No_alk in Fig. 3).
567 For Sand 2, Δ Alkalinity was about 85 $\mu\text{mol/kg}$ higher in one replicate bottle than in the other two. This difference
568 was due to a small arthropod (likely a sand flea) that was unintentionally added to the incubation bottle with the
569 high Δ Alkalinity. The arthropod was still alive at the end of the 6.8 incubation period. During those 6.8 days, the
570 organism respired, thereby reducing Ω_{Ara} , and causing alkalinity release from the sand via CaCO_3 dissolution.
571 This observation pointed out that the baseline system can already release substantial amounts of alkalinity even
572 before OAE is implemented given sufficient respiration. Indeed, the in-situ observations at Clifton South suggest
573 that alkalinity release occurs in the baseline system used here (section 3.1). Furthermore, there is widespread
574 evidence from the literature that beaches release alkalinity via CaCO_3 dissolution (Liu et al., 2021; Perkins et al.,
575 2022; Reckhardt et al., 2015). These insights collectively inspired Experiment 2, where a DIC gradient (high to
576 low Ω_{Ara}) was set up to test if natural alkalinity release via CaCO_3 dissolution would be influenced by
577 anthropogenic alkalinity release via OAE.

578 Experiment 2 demonstrated that the release of natural alkalinity can be disturbed by the addition of anthropogenic
579 alkalinity sources (Fig. 7). Fig. 7A illustrates the additionality of alkalinity release, calculated by subtracting
580 Δ Alkalinity from sand-only incubations (represented by the orange lines in Fig. 4 panels A-D) from Δ Alkalinity
581 in sand+alkalinity incubations (represented by the red and blue lines). Fig. 7A reveals that the additionality of
582 Δ Alkalinity declines with increasing amounts of added DIC. The reason for this trend is that the alkalinity sources
583 added to the incubation bottles buffered the DIC-induced pH decline. This buffering elevated Ω_{Ara} during the
584 incubations, resulting in a reduced release of natural alkalinity through CaCO_3 dissolution. Or in simpler terms,
585 by adding a new buffer system via OAE (NaOH, slag, or olivine), a natural buffer system (CaCO_3 dissolution) is
586 partially replaced. In cases where olivine or non-equilibrated NaOH was tested, the additionality of Δ Alkalinity
587 became even negative when DIC additions were >350 and >400 $\mu\text{mol/kg}$, respectively (Fig. 7A).

588 Alkalinity release is generally seen as a good indicator for the amount of CO_2 that can be removed per mole
589 alkalinity enhancement (η_{CO_2}). However, as discussed in section 4.1., η_{CO_2} also critically depends on whether the
590 released alkalinity is $\text{Alk}_{\text{carbonate}}$ or $\text{Alk}_{\text{non-carbonate}}$. In Experiment 2, η_{CO_2} varies greatly depending on the alkalinity
591 source and the amount of DIC added to the incubation (Fig. 7B). η_{CO_2} is low for sand-only incubations because
592 basically all Δ Alkalinity is $\text{Alk}_{\text{carbonate}}$, whereas it is substantially higher in treatments with an anthropogenic
593 $\text{Alk}_{\text{non-carbonate}}$ source. For olivine, η_{CO_2} was around 0.7 mol:mol up until the highest DIC additions where η_{CO_2}
594 declines slightly. This is lower than for slag, where η_{CO_2} remains close to the theoretical maximum of 0.86
595 mol:mol. The difference between slag and olivine could be due to faster dissolution of slag, which elevates Ω_{Ara}
596 before substantial CaCO_3 dissolution had occurred. In contrast, olivine dissolves more slowly (Fuhr et al., 2022;
597 Montserrat et al., 2017), so that some CaCO_3 dissolution may have occurred before olivine dissolution elevated
598 Ω_{Ara} enough to limit further CaCO_3 dissolution. (Please note, however, that this explanation does not explain why
599 η_{CO_2} is also lower than in slag incubations at low DIC additions, where Ω_{Ara} was low enough to limit CaCO_3
600 dissolution from the start). The reason for the decreasing η_{CO_2} in the equilibrated NaOH scenario (Fig. 7B) is an
601 increasing contribution of $\text{Alk}_{\text{carbonate}}$ to Δ Alkalinity. It is important to note that for the same added DIC, Ω_{Ara} is
602 much lower in the equilibrated NaOH scenario than in unequilibrated NaOH scenario (e.g. 0.28 vs. 2.9 at ~ 400
603 $\mu\text{mol/kg}$ added DIC for the equilibrated and unequilibrated NaOH scenarios, respectively). This lower Ω_{Ara} in the
604 equilibrated scenario is due to atmospheric CO_2 in-gassing, which has already reduced Ω_{Ara} in the equilibrated



605 scenario before this seawater starts interacting with beach sediments rich in respiratory CO_2 . As such, this OAE
606 scenario causes less reduction of natural alkalinity release from sediments via CaCO_3 dissolution.
607 Measurements and estimates of $\Delta\text{Alkalinity}$ and η_{CO_2} enabled calculation of how much DIC could be maximally
608 stored by the generated alkalinity (i.e., DIC_{OAE} shown in Fig. 7C). DIC_{OAE} increases with higher DIC additions
609 due to the release of alkalinity via CaCO_3 dissolution. However, the increase is less pronounced as observed for
610 $\Delta\text{Alkalinity}$ (Fig. 7A) because $\text{Alk}_{\text{carbonate}}$ from CaCO_3 dissolution is less efficient in sequestering environmental
611 CO_2 than $\text{Alk}_{\text{non-carbonate}}$ from NaOH, slag, or olivine (section 4.1).
612 To calculate the additionality of DIC_{OAE} , I subtracted DIC_{OAE} of the sand-only incubations (baseline) of DIC_{OAE}
613 of the OAE scenarios (Fig. 7D). The additionality of DIC_{OAE} is arguably the most important parameter to assess
614 whether an OAE deployment has led to the net sequestration of CO_2 . In the case of the equilibrated NaOH and
615 slag scenarios, the additionality of DIC_{OAE} was constant over the applied gradient, suggesting that the release of
616 $\text{Alk}_{\text{carbonate}}$ via CaCO_3 dissolution led to similar DIC_{OAE} potential in the sand-only scenario and these two OAE
617 scenarios. In contrast, the additionality of DIC_{OAE} declined in the olivine scenario because there was relatively
618 more $\text{Alk}_{\text{carbonate}}$ release in the sand only scenario than in the olivine scenario (Fig. 7D). Importantly, however, the
619 additionality of DIC_{OAE} remains positive up until the highest DIC addition, which is in stark contrast to the
620 additionality of $\Delta\text{Alkalinity}$ (compare Fig 7A and D). This means that the addition of olivine maintained a positive
621 CO_2 sequestration potential even though less alkalinity was generated in the olivine treatment than in the sand-
622 only treatment (Fig. 7C). The reason for this counterintuitive observation is simply that the $\text{Alk}_{\text{non-carbonate}}$ released
623 by olivine has more potential to sequester CO_2 than the $\text{Alk}_{\text{carbonate}}$ released via CaCO_3 dissolution.
624



625

626 **Figure 7.** Various measures of OAE efficiency under increasing additions of DIC (DIC could for example be CO₂
627 from the respiration of organic material in sediments). (A) The additionality of ΔAlkalinity. (B) η_{CO_2} at the end
628 of the experiment. (C) DIC_{OAE}, i.e., how much seawater CO₂ could have potentially been absorbed with the
629 amount of ΔAlkalinity provided by the various alkalinity sources. (D) The additionality of DIC_{OAE}. Please note
630 that panels (B-D) only show data for the equilibrated NaOH scenario. I omitted the unequilibrated scenario for
631 logical reasons, i.e., because the core assumption in this scenario (no CO₂ equilibration with the atmosphere after
632 OAE) is at odds with the necessary assumption of CO₂ equilibration to calculate η_{CO_2} (see eq. 10).

633

634 4.2.3. Relevance of the additionality problem of OAE and possible solutions

635

636 Modifications of additionality can occur when OAE triggers subsequent alkalinity loss through biotic and abiotic
637 carbonate precipitation (section 4.2.1.). This feedback has been widely discussed and is already a predominant
638 topic in OAE research (Bach et al., 2019; Fuhr et al., 2022; Hartmann et al., 2013, 2023; Moras et al., 2022). Not
639 yet discussed is the modification of additionality that may occur when anthropogenic alkalinity sources (via OAE)
640 modify the release of natural alkalinity (section 4.2.2.). Thus, I will focus on the relevance of this second pathway
641 of additionality modification in the following.

642 The experiments conducted here tested mineral dissolution feedbacks with beach sand and in a setting that
643 assumes constant mixing, comparable to a high energy wave impact zone. This setting was chosen based on the
644 widely discussed OAE implementation strategy adding olivine powder to beaches. The results suggest that the



645 “additionality problem” needs to be considered for this specific OAE approach. However, the wave impact zone
646 comprises a tiny fraction of the coastal ocean and the question is to what extent the additionality problem also
647 applies to the vast shelf, bank, embayment and reef areas where OAE could also be implemented (Feng et al.,
648 2017; Meysman and Montserrat, 2017; Mongin et al., 2021). The coastal ocean is a net sink of ~ 36 Tmol/year
649 alkalinity via CaCO_3 burial (Middelburg et al., 2020), but considerable amounts of alkalinity are also generated
650 in the various coastal sediments via CaCO_3 dissolution (one estimate suggests ~ 13 Tmol/year; (Krumins et al.,
651 2013)). The dissolution depends on the solubility of CaCO_3 present in the sediments and pore water Ω
652 (Middelburg et al., 2020). Conditions for dissolution are generally favourable in coastal ocean sediments because
653 soluble forms of CaCO_3 occur more frequently and relatively high supply of organic matter lowers Ω_{CaCO_3}
654 (Krumins et al., 2013; Lunstrum and Berelson, 2022; Morse et al., 1985). Thus, the introduction of an
655 anthropogenic buffer via OAE (which increases Ω_{CaCO_3}) is likely to cause a reduction of alkalinity release from
656 the seafloor.

657 Indeed, more soluble forms of CaCO_3 were shown to protect less soluble forms of CaCO_3 from
658 dissolution at the seafloor (Sulpis et al., 2022). Furthermore, an experiment exposed a coral reef to moderate levels
659 of increased alkalinity ($\Delta\text{Alkalinity} = \sim 50 \mu\text{mol/kg}$) and found a net increase of reef calcification, with some
660 evidence suggesting that the measured effect was due to reduced reef dissolution (Albright et al., 2016).
661 Anthropogenic alkalinity sources (e.g. NaOH, slag, olivine) introduced via OAE can be considered to have a
662 similar effect and reduce natural alkalinity release via CaCO_3 dissolution. It is worth noting that the negative effect
663 of anthropogenic alkalinity on natural alkalinity release may also occur in the open surface ocean. Here, part of
664 the alkalinity bound in particulate form via biotic calcification re-dissolves, for example in corrosive
665 microenvironments such as zooplankton or marine snow (Milliman et al., 1999; Subhas et al., 2022; Sulpis et al.,
666 2021). If anthropogenic alkalinity introduced via OAE reduces this natural dissolution of CaCO_3 in the surface
667 ocean, then less alkalinity would remain in the surface ocean and the additionality of OAE would be reduced
668 (Bach et al., 2019). Thus, the “additionality problem” of OAE could be widespread and not restricted to the
669 specific environment studied experimentally in this paper.

670 To manage the additionality problem, it is important to monitor the natural alkalinity release in a designated OAE
671 deployment site before OAE is implemented. Natural alkalinity release occurs in all coastal habitats (Aller, 1982;
672 Krumins et al., 2013; Liu et al., 2021; Perkins et al., 2022) and recent evidence suggests that even small CaCO_3
673 content in sediments is sufficient to yield high alkalinity release rates (Lunstrum and Berelson, 2022). As such,
674 dissolution is not restricted to CaCO_3 rich sediments and avoiding these may therefore not mitigate the
675 additionality problem. More crucial than the CaCO_3 content appears to be the supply of organic matter to the
676 seafloor, which enhances alkalinity release through the supply of respiratory CO_2 (Aller, 1982; Krumins et al.,
677 2013; Liu et al., 2021; Lunstrum and Berelson, 2022; Perkins et al., 2022). Therefore, it may be useful to avoid
678 OAE near sediments exposed to high organic matter load to reduce the interference of anthropogenic alkalinity
679 with natural alkalinity release.

680 Another mitigation pathway for the additionality problem is dilution. When anthropogenic alkalinity is diluted
681 quickly then there is less chance for the new buffer system to generate oversaturated Ω in seawater, sediment pore
682 waters, or other microenvironments. The experiments presented here do not allow for such dilution as they are
683 performed in enclosed volumes. They can therefore be considered a more extreme case, which do not correctly
684 represent the vastness of the ocean and its volume. Indeed, previous experiments investigating the risk of alkalinity





685 loss after OAE due to secondary precipitation found that dilution effectively mitigates the secondary precipitation
686 problem (Moras et al., 2022). It is very likely that dilution is similarly effective to mitigate the additionality
687 problem.

688 Finally, the data presented here clearly shows that the additionality problem scales with the degree of CaCO_3
689 oversaturation introduced through the anthropogenic alkalinity source. This is most obvious when comparing the
690 equilibrated with the unequilibrated NaOH OAE scenario. The increase of Ω_{CaCO_3} is much more pronounced in
691 the unequilibrated scenario because atmospheric CO_2 has not yet entered the seawater and brought down Ω_{CaCO_3}
692 to levels it was before the OAE perturbation. As such, the additionality problem will be much more pronounced
693 when an alkalinity source interacts with naturally alkalinity releasing sediments before the OAE-perturbed
694 seawater has been equilibrated with atmospheric CO_2 . Nevertheless, a close look at Fig. 3A (equilibrated NaOH)
695 shows that even the relatively small increase of Ω_{CaCO_3} that coincides with OAE fully equilibrated with
696 atmospheric CO_2 , can reduce natural alkalinity release. Thus, atmospheric CO_2 equilibration following OAE
697 mitigates the additionality problem but cannot fully avoid it.

698

699 5. Conclusion and outlook

700

701 The additionality problem described herein could influence the effectiveness of OAE. It suggests that interference
702 of anthropogenic alkalinity with the natural alkalinity cycle must be assessed as a factor that can modify the OAE
703 efficiency. The arguments provided in the discussion suggest that the additionality problem is potentially
704 widespread, even though the dataset presented here only considers OAE near or on wave-exposed beaches. Future
705 research should aim to confirm or dismiss these arguments and to better understand the extent of the problem.

706 The additionality problem adds a layer of complexity to monitoring, reporting, and verification of CO_2 removal
707 with OAE. Strictly speaking, it is not sufficient to monitor the generation (e.g., via NaOH, slag, or olivine
708 dissolution) and potential loss (e.g., via biotic and abiotic precipitation) of anthropogenic alkalinity after its
709 generation. It also needs to be assessed to what extent anthropogenic alkalinity alters the baseline removal or
710 delivery of natural alkalinity. It will be crucial to understand whether the anthropogenic acceleration of the
711 alkalinity cycle in the oceans via OAE could slow down the natural alkalinity cycle.

712



713 Competing interests

714 The author declares no competing interests.

715

716 Acknowledgements

717 I thank Jiaying Guo and Bec Lenc for providing particle size spectra, the Mortlake Council for providing olivine
718 samples, Bradley Mansell from Liberty Primary Steel for providing steel slag aggregates, and the Central Science
719 Laboratory at the University of Tasmania for particulate carbon analyses. This research was funded through a
720 Future Fellowship Award by the Australian Research Council (FT200100846) and by the Carbon-to-Sea
721 Initiative, a non-profit dedicated to evaluate Ocean Alkalinity Enhancement.

722

723 Data availability statement



724 All data and evaluation scripts (for R) generated herein are available for download at zenodo.org under the
725 doi:10.5281/zenodo.8191516.

726

727

728 **References**

- 729 Albright, R., Caldeira, L., Hoffelt, J., Kwiatkowski, L., Maclaren, J. K., Mason, B. M., Nebuchina, Y.,
730 Ninokawa, A., Pongratz, J., Ricke, K. L., Rivlin, T., Schneider, K., Sesboté, M., Shamberger, K., Silverman, J.,
731 Wolfe, K., Zhu, K. and Caldeira, K.: Reversal of ocean acidification enhances net coral reef calcification,
732 *Nature*, 531(7594), 362–365, doi:10.1038/nature17155, 2016.
- 733 Aller, R. C.: Carbonate Dissolution in Nearshore Terrigenous Muds: The Role of Physical and Biological
734 Reworking, *J. Geol.*, 90(1), 79–95, doi:10.1086/628652, 1982.
- 735 Bach, L. T., Gill, S. J., Rickaby, R. E. M., Gore, S. and Renforth, P.: CO₂ Removal With Enhanced Weathering
736 and Ocean Alkalinity Enhancement: Potential Risks and Co-benefits for Marine Pelagic Ecosystems, *Front.*
737 *Clim.*, 1(October), 1–21, doi:10.3389/fclim.2019.00007, 2019.
- 738 Caserini, S., Storni, N. and Grosso, M.: The Availability of Limestone and Other Raw Materials for Ocean
739 Alkalinity Enhancement, *Global Biogeochem. Cycles*, 36(5), doi:10.1029/2021GB007246, 2022.
- 740 Dickson, A. G., Afghan, J. D. and Anderson, G. C.: Reference materials for oceanic CO₂ analysis: a method for
741 the certification of total alkalinity, *Mar. Chem.*, 80(2–3), 185–197, doi:10.1016/S0304-4203(02)00133-0, 2003.
- 742 Dickson, A. G., Sabine, C. L. and Christian, J. R.: Guide to Best Practices for Ocean CO₂ Measurements,
743 *PICES Spec.*, PICES, Sidney., 2007.
- 744 Eisaman, M. D., Rivest, J. L. B., Karnitz, S. D., Lannoy, C. De, Jose, A., Devaul, R. W. and Hannun, K.:
745 *International Journal of Greenhouse Gas Control Indirect ocean capture of atmospheric CO₂: Part II .*
746 *Understanding the cost of negative emissions*, *Int. J. Greenh. Gas Control*, 70(May 2017), 254–261,
747 doi:10.1016/j.ijggc.2018.02.020, 2018.
- 748 Eisaman, M. D., Geilert, S., Renforth, P., Bastianini, L., Campbell, J., Dale, A. W., Foteinis, S., Grasse, P.,
749 Hawrot, O., Löscher, C. R., Rau, G. H. and Rønning, J.: Chapter 3: Assessing the technical aspects of OAE
750 approaches, in *Guide for best practices in Ocean Alkalinity Enhancement.*, 2023.
- 751 Fakhraee, M., Planavsky, N. J. and Reinhard, C. T.: Ocean alkalinity enhancement through restoration of blue
752 carbon ecosystems, *Nat. Sustain.*, doi:10.1038/s41893-023-01128-2, 2023.
- 753 Feng, E. Y., Koeve, W., Keller, D. P. and Oschlies, A.: Model-Based Assessment of the CO₂ Sequestration
754 Potential of Coastal Ocean Alkalinization, *Earth's Futur.*, 5, 1252–1266, doi:10.1002/ef2.273, 2017.
- 755 Ferderer, A., Chase, Z., Kennedy, F., Schulz, K. G. and Bach, L. T.: Assessing the influence of ocean alkalinity
756 enhancement on a coastal phytoplankton community, *Biogeosciences*, 19(23), 5375–5399, doi:10.5194/bg-19-
757 5375-2022, 2022.
- 758 Fuhr, M., Geilert, S., Schmidt, M., Liebetrau, V., Vogt, C., Ledwig, B. and Wallmann, K.: Kinetics of Olivine
759 Weathering in Seawater: An Experimental Study, *Front. Clim.*, 4(March), 1–20,
760 doi:10.3389/fclim.2022.831587, 2022.
- 761 Gattuso, J.-P., Epitalon, J.-M., Lavigne, H. and Orr, J.: Seacarb: seawater carbonate chemistry with R. R
762 package version 3.0, [online] Available from: <http://cran.r-project.org/package=seacarb>, 2021.
- 763 Hansen, H. P. and Koroleff, F.: Determination of nutrients, in *Methods of Seawater Analysis*, edited by K.



- 764 Grasshoff, K. Kremling, and M. Ehrhardt, pp. 159–226, Wiley-VCH, Weinheim., 1999.
- 765 Hartmann, J., West, a J., Renforth, P., Köhler, P., Rocha, C. L. D. La, Wolf-gladrow, D. a, Dürr, H. H. and
766 Scheffran, J.: Enhanced chemical weathering as a geoengineering strategy to reduce atmospheric carbon
767 dioxide, supply nutrients, and mitigate ocean acidification, *Rev. Geophys.*, 51(2012), 113–149,
768 doi:10.1002/rog.20004.1.Institute, 2013.
- 769 Hartmann, J., Suitner, N., Lim, C., Schneider, J., Marin-Samper, L., Aristegui, J., Renforth, P., Taucher, J. and
770 Riebesell, U.: Stability of alkalinity in ocean alkalinity enhancement (OAE) approaches - consequences for
771 durability of CO₂ storage, *Biogeosciences*, 20(4), 781–802, doi:10.5194/bg-20-781-2023, 2023.
- 772 Harvey, L. D. D.: Mitigating the atmospheric CO₂ increase and ocean acidification by adding limestone powder
773 to upwelling regions, *J. Geophys. Res. Ocean.*, 113(4), 1–21, doi:10.1029/2007JC004373, 2008.
- 774 He, J. and Tyka, M. D.: Limits and CO₂ equilibration of near-coast alkalinity enhancement, *Biogeosciences*, 20,
775 27–43, doi:10.5194/bg-20-27-2023, 2023.
- 776 Humphreys, M. P., Gregor, L., Pierrot, D., van Heuven, S. M. A. C., Lewis, E. R. and Wallace, D. W. R.:
777 PyCO₂SYs: marine carbonate system calculations in Python, , doi:10.5281/zenodo.3744275, 2020.
- 778 Krumins, V., Gehlen, M., Arndt, S., Van Cappellen, P. and Regnier, P.: Dissolved inorganic carbon and
779 alkalinity fluxes from coastal marine sediments: Model estimates for different shelf environments and
780 sensitivity to global change, *Biogeosciences*, 10(1), 371–398, doi:10.5194/bg-10-371-2013, 2013.
- 781 de Lannoy, C. F., Eisaman, M. D., Jose, A., Karnitz, S. D., DeVaul, R. W., Hannun, K. and Rivest, J. L. B.:
782 Indirect ocean capture of atmospheric CO₂: Part I. Prototype of a negative emissions technology, *Int. J. Greenh.*
783 *Gas Control*, 70(May 2017), 243–253, doi:10.1016/j.ijggc.2017.10.007, 2018.
- 784 Lezaun, J.: Hugging the Shore: Tackling Marine Carbon Dioxide Removal as a Local Governance Problem,
785 *Front. Clim.*, 3(August), 1–6, doi:10.3389/fclim.2021.684063, 2021.
- 786 Liu, Y., Jiao, J. J., Liang, W., Santos, I. R., Kuang, X. and Robinson, C. E.: Inorganic carbon and alkalinity
787 biogeochemistry and fluxes in an intertidal beach aquifer: Implications for ocean acidification, *J. Hydrol.*,
788 595(January), 126036, doi:10.1016/j.jhydrol.2021.126036, 2021.
- 789 Lueker, T. J., Dickson, A. G. and Keeling, C. D.: Ocean pCO₂ calculated from dissolved inorganic carbon,
790 alkalinity, and equations for K₁ and K₂: Validation based on laboratory measurements of CO₂ in gas and
791 seawater at equilibrium, *Mar. Chem.*, 70, 105–119, doi:10.1016/S0304-4203(00)00022-0, 2000.
- 792 Lunstrum, A. and Berelson, W.: CaCO₃ dissolution in carbonate-poor shelf sands increases with ocean
793 acidification and porewater residence time, *Geochim. Cosmochim. Acta*, 329, 168–184,
794 doi:10.1016/j.gca.2022.04.031, 2022.
- 795 Meysman, F. J. R. and Montserrat, F.: Negative CO₂ emissions via enhanced silicate weathering in coastal
796 environments, *Biol. Lett.*, 13(4), 20160905, doi:10.1098/rsbl.2016.0905, 2017.
- 797 Middelburg, J. J., Soetaert, K. and Hagens, M.: Ocean Alkalinity, Buffering and Biogeochemical Processes,
798 *Rev. Geophys.*, 58(3), doi:10.1029/2019RG000681, 2020.
- 799 Milliman, J. D., Troy, P. J., Balch, W. M., Adams, a. K., Li, Y.-H. and Mackenzie, F. T.: Biologically mediated
800 dissolution of calcium carbonate above the chemical lysocline?, *Deep Sea Res. Part I Oceanogr. Res. Pap.*,
801 46(10), 1653–1669, doi:10.1016/S0967-0637(99)00034-5, 1999.
- 802 Mongin, M., Baird, M. E., Lenton, A., Neill, C. and Akl, J.: Reversing ocean acidification along the Great
803 Barrier Reef using alkalinity injection, *Environ. Res. Lett.*, 16(6), doi:10.1088/1748-9326/ac002d, 2021.



- 804 Montserrat, F., Renforth, P., Hartmann, J., Leermakers, M., Knops, P. and Meysman, F. J. R.: Olivine
805 Dissolution in Seawater: Implications for CO₂ Sequestration through Enhanced Weathering in Coastal
806 Environments, *Environ. Sci. Technol.*, 51(7), 3960–3972, doi:10.1021/acs.est.6b05942, 2017.
- 807 Moras, C. A., Bach, L. T., Cyronak, T., Joannes-Boyau, R. and Schulz, K. G.: Ocean alkalinity enhancement -
808 avoiding runaway CaCO₃ precipitation during quick and hydrated lime dissolution, *Biogeosciences*, 19(15),
809 3537–3557, doi:10.5194/bg-19-3537-2022, 2022.
- 810 Morse, J. W., Zullig, J. J., Bernstein, L. D., Millero, F. J., Milne, P., Mucci, A. and Choppin, G. R.: Chemistry
811 of calcium carbonate-rich shallow water sediments in the Bahamas., *Am. J. Sci.*, 285(2), 147–185,
812 doi:10.2475/ajs.285.2.147, 1985.
- 813 Morse, J. W., Gledhill, D. K. and Millero, F. J.: CaCO₃ precipitation kinetics in waters from the great Bahama
814 bank: Implications for the relationship between bank hydrochemistry and whittings, *Geochim. Cosmochim.*
815 *Acta*, 67(15), 2819–2826, doi:10.1016/S0016-7037(03)00103-0, 2003.
- 816 Mucci, A.: The solubility of calcite and aragonite in seawater at various salinities, temperatures, and one
817 atmosphere total pressure, *Am. J. Sci.*, 283(7), 780–799, 1983.
- 818 Nemet, G. F., Callaghan, M. W., Creutzig, F., Fuss, S., Hartmann, J., Hilaire, J., Lamb, W. F., Minx, J. C.,
819 Rogers, S. and Smith, P.: Negative emissions — Part 3: Innovation and upscaling, *Environ. Res. Lett.*, 13,
820 06300, 2018.
- 821 Oelkers, E. H., Declercq, J., Saldi, G. D., Gislason, S. R. and Schott, J.: Olivine dissolution rates: A critical
822 review, *Chem. Geol.*, 500(October), 1–19, doi:10.1016/j.chemgeo.2018.10.008, 2018.
- 823 Perkins, A. K., Santos, I. R., Rose, A. L., Schulz, K. G., Grossart, H. P., Eyre, B. D., Kelaher, B. P. and Oakes,
824 J. M.: Production of dissolved carbon and alkalinity during macroalgal wrack degradation on beaches: a
825 mesocosm experiment with implications for blue carbon, *Biogeochemistry*, 160(2), 159–175,
826 doi:10.1007/s10533-022-00946-4, 2022.
- 827 Rau, G. H. and Caldeira, K.: Enhanced carbonate dissolution: A means of sequestering waste CO₂ as ocean
828 bicarbonate, *Energy Convers. Manag.*, 40(17), 1803–1813, doi:10.1016/S0196-8904(99)00071-0, 1999.
- 829 Reckhardt, A., Beck, M., Seidel, M., Riedel, T., Wehrmann, A., Bartholomä, A., Schnetger, B., Dittmar, T. and
830 Brumsack, H. J.: Carbon, nutrient and trace metal cycling in sandy sediments: A comparison of high-energy
831 beaches and backbarrier tidal flats, *Estuar. Coast. Shelf Sci.*, 159, 1–14, doi:10.1016/j.ecss.2015.03.025, 2015.
- 832 Renforth, P.: The negative emission potential of alkaline materials, *Nat. Commun.*, 10, doi:10.1038/s41467-
833 019-09475-5, 2019.
- 834 Renforth, P. and Henderson, G.: Assessing ocean alkalinity for carbon sequestration, *Rev. Geophys.*, 55(3),
835 636–674, doi:10.1002/2016RG000533, 2017.
- 836 Renforth, P., Baltruschat, S., Peterson, K., Mihailova, B. D. and Hartmann, J.: Using ikaite and other hydrated
837 carbonate minerals to increase ocean alkalinity for carbon dioxide removal and environmental remediation,
838 *Joule*, 6(12), 2674–2679, doi:10.1016/j.joule.2022.11.001, 2022.
- 839 Saderne, V., Fusi, M., Thomson, T., Dunne, A., Mahmud, F., Roth, F., Carvalho, S. and Duarte, C. M.: Total
840 alkalinity production in a mangrove ecosystem reveals an overlooked Blue Carbon component, *Limnol.*
841 *Oceanogr. Lett.*, 6(2), 61–67, doi:10.1002/lo12.10170, 2021.
- 842 Schuiling, R. D. and de Boer, P. L.: Rolling stones; fast weathering of olivine in shallow seas for cost-effective
843 CO₂ capture and mitigation of global warming and ocean acidification, *Earth Syst. Dyn. Discuss.*, 2, 551–568,



- 844 doi:10.5194/esdd-2-551-2011, 2011.
- 845 Schuiling, R. D. and Krijgsman, P.: Enhanced weathering: An effective and cheap tool to sequester CO₂, *Clim.*
- 846 *Change*, 74(1–3), 349–354, doi:10.1007/s10584-005-3485-y, 2006.
- 847 Schulz, K. G., Bach, L. T. and Dickson, A. G.: Seawater carbonate system considerations for ocean alkalinity
- 848 enhancement research, *Guid. best Pract. Ocean Alkalinity Enhanc.*, 2023.
- 849 Shi, C.: Steel Slag—Its Production, Processing, Characteristics, and Cementitious Properties, *J. Mater. Civ.*
- 850 *Eng.*, 16(3), 230–236, doi:10.1061/(asce)0899-1561(2004)16:3(230), 2004.
- 851 Subhas, A. V., Dong, S., Naviaux, J. D., Rollins, N. E., Ziveri, P., Gray, W., Rae, J. W. B., Liu, X., Byrne, R.
- 852 H., Chen, S., Moore, C., Martell-Bonet, L., Steiner, Z., Antler, G., Hu, H., Lunstrum, A., Hou, Y., Kemnitz, N.,
- 853 Stutsman, J., Pallacks, S., Dugenne, M., Quay, P. D., Berelson, W. M. and Adkins, J. F.: Shallow Calcium
- 854 Carbonate Cycling in the North Pacific Ocean, *Global Biogeochem. Cycles*, 36(5), 1–22,
- 855 doi:10.1029/2022GB007388, 2022.
- 856 Sulpis, O., Jeansson, E., Dinauer, A., Lauvset, S. K. and Middelburg, J. J.: Calcium carbonate dissolution
- 857 patterns in the ocean, *Nat. Geosci.*, 14(6), 423–428, doi:10.1038/s41561-021-00743-y, 2021.
- 858 Sulpis, O., Agrawal, P., Wolthers, M., Munhoven, G., Walker, M. and Middelburg, J. J.: Aragonite dissolution
- 859 protects calcite at the seafloor, *Nat. Commun.*, 13(1), 1–8, doi:10.1038/s41467-022-28711-z, 2022.
- 860 Tyka, M. D., Van Arsdale, C. and Platt, J. C.: CO₂ capture by pumping surface acidity to the deep ocean, *Energy*
- 861 *Environ. Sci.*, 15(2), 786–798, doi:10.1039/d1ee01532j, 2022.
- 862 Wallmann, K., Diesing, M., Scholz, F., Rehder, G., Dale, A. W., Fuhr, M. and Suess, E.: Erosion of carbonate-
- 863 bearing sedimentary rocks may close the alkalinity budget of the Baltic Sea and support atmospheric CO₂
- 864 uptake in coastal seas, *Front. Mar. Sci.*, 9(September), 1–15, doi:10.3389/fmars.2022.968069, 2022.
- 865 Zhong, S. and Mucci, A.: Calcite and aragonite precipitation from seawater solutions of various salinities:
- 866 Precipitation rates and overgrowth compositions, *Chem. Geol.*, 78, 283–299, doi:10.1016/0009-2541(89)90064-
- 867 8, 1989.
- 868